

# Anomalous production of top quarks at CLIC+LHC based $\gamma p$ colliders

Orhan Çakır\*

Ankara University, Faculty of Sciences, Department of Physics, 06100, Tandogan, Ankara, Turkey.

The single production of top quark due to flavor changing neutral current (FCNC) interaction and its decay to  $bW$  are studied at CLIC+LHC based  $\gamma p$  colliders. We consider both  $tc\gamma$  and  $tu\gamma$  anomalous couplings. The anomalous charm (up) quark anomalous coupling parameter  $\kappa_\gamma^c$  ( $\kappa_\gamma^u$ ) can be probed down to  $9.5 \times 10^{-3}$  ( $8.0 \times 10^{-3}$ ) at a  $\gamma p$  collider with  $\sqrt{s_{ep}} = 6.48$  TeV and  $L_{\text{int}} = 100$  fb $^{-1}$ .

The flavor changing neutral current (FCNC) reactions are known to be absent at tree level in the Standard Model (SM). However, they can naturally appear at the one-loop level due to CKM mixing which leads to the branching ratio  $\text{BR}(t \rightarrow qV) \sim 10^{-13} - 10^{-10}$  [1] where  $q = c, u$  and  $V = \gamma, g, Z$ . Extensions of the SM such as supersymmetry (SUSY) [2], exotic quarks (EXQ) [3],[4] and two-Higgs doublet models (2HDM) [5] could lead to an enhancements of such transitions. In these models the top quark is predicted to have large FCNC couplings [6, 7]. The approximate orders of the branching ratios for FCNC top quark decays predicted within these models [see [8] and references therein] are given in Table I.

Due to the large mass close to the electroweak symmetry breaking scale and having poorly measured couplings, the top quark is a good candidate for probing new physics beyond the SM. This motivates the study of single top production by FCNC couplings at future colliders. The production of top quarks via FCNC interactions was extensively studied at hadron colliders [9, 10, 11, 12, 13, 14, 15], at  $e^+e^-$  colliders [15, 16, 17, 18], and at lepton-hadron colliders [18, 19].

Additional option of linear  $e^+e^-$  colliders would be an ep collider when linear collider is constructed on the same base as the proton ring. The compact linear collider (CLIC) [20] at CERN can be converted into CLIC+LHC ep collider. Photon colliders [21] are based on the Compton scattering of laser light on high energy electrons in linear colliders. The scattered photons have energies close to the energy of the initial electron beams. Then, it is possible to construct TeV scale  $\gamma p$  collider on the CLIC+LHC base. The main parameters of the CLIC+LHC based  $\gamma p$  colliders are given in Table II.

In this paper, single production of top quarks via anomalous  $tc\gamma$  and  $tu\gamma$  couplings at future CLIC+LHC based  $\gamma p$  colliders has been studied.

If the FCNC couplings of the top quark exist, they will affect top quark production and decay at high energies. Therefore, any possible deviations from SM predictions will be an indication of new physics. Top quark FCNC couplings can be parametrized in a model independent way by an effective Lagrangian

$$\begin{aligned}
 L = & \sum_{q=u,c} ig_e Q_q \frac{\kappa_\gamma^q}{\Lambda} \bar{t} \sigma_{\mu\nu} k^\nu q A^\mu \\
 & + \sum_{q=u,c} \frac{g_e}{2 \sin \theta_W \cos \theta_W} \bar{t} \left[ i \frac{\kappa_Z^q}{\Lambda} \sigma_{\mu\nu} k^\nu - \gamma_\mu (v_Z^q - a_Z^q \gamma_5) \right] q Z^\mu \\
 & + \sum_{q=u,c} ig_s \frac{\kappa_g^q}{\Lambda} \bar{t} \sigma_{\mu\nu} k^\nu \frac{\lambda^a}{2} q G_a^\mu + \text{H.c.}
 \end{aligned} \tag{1}$$

where  $k^\nu$  is the momentum of the neutral gauge boson,  $\sigma_{\mu\nu} = i(\gamma_\mu \gamma_\nu - \gamma_\nu \gamma_\mu)/2$  and  $\Lambda$  is the new physics scale.  $A^\mu$ ,  $Z^\mu$  and  $G^\mu$  are the photon, Z- boson and gluon fields, respectively. The anomalous couplings  $\kappa_\gamma$ ,  $\kappa_Z$  ve  $\kappa_g$  define the strength of the  $tq\gamma$ ,  $tqZ$  and  $tqg$  vertices, respectively. The terms including  $v_Z$  and  $a_Z$  are the anomalous non-diagonal Z couplings which are zero in the SM.  $g_e$  and  $g_s$  are the electromagnetic and strong coupling constants, respectively.  $Q_q$  is the quark charge and  $\theta_W$  is the Weinberg angle.

Using the effective Lagrangian (1) it is straightforward to obtain the FCNC decay widths of top quark:

$$\Gamma(t \rightarrow qg) = \left( \frac{\kappa_g^q}{\Lambda} \right)^2 \frac{2}{3} \alpha_s m_t^3 \tag{2}$$

---

\*Electronic address: ocakir@science.ankara.edu.tr; URL: <http://science.ankara.edu.tr/~ocakir>

$$\Gamma(t \rightarrow q\gamma) = \left(\frac{\kappa_\gamma^q}{\Lambda}\right)^2 \frac{2}{9} \alpha m_t^3 \quad (3)$$

$$\Gamma(t \rightarrow qZ) = \frac{\alpha m_t}{4 \sin^2 2\theta_W} \left(1 - \frac{m_Z^2}{m_t^2}\right)^2 \left[ \left(\frac{\kappa_Z^q}{\Lambda}\right)^2 m_t^2 \left(2 + \frac{m_Z^2}{m_t^2}\right) - 6v_Z^q \frac{\kappa_Z^q}{\Lambda} m_t + (v_Z^{q2} + a_Z^{q2}) \left(2 + \frac{m_t^2}{m_Z^2}\right) \right] \quad (4)$$

where  $m_Z$  and  $m_t$  are the masses of Z boson and top quark, respectively.

The CDF collaboration performed a search for FCNC in the top quark decays  $t \rightarrow u(c)\gamma$  and  $t \rightarrow u(c)Z$  in  $p\bar{p}$  collisions at a centre of mass energy of 1.8 TeV. They obtained upper limits at 95% confidence level (CL) on the branching ratios [22]:

$$BR(t \rightarrow u\gamma) + BR(t \rightarrow c\gamma) < 0.032,$$

$$BR(t \rightarrow uZ) + BR(t \rightarrow cZ) < 0.33.$$

A slightly better limit from the DELPHI experiments for the process  $e^+e^- \rightarrow t\bar{q}$  is obtained on the top quark FCNC branching fraction  $BR(t \rightarrow uZ) + BR(t \rightarrow cZ) < 0.18$  [23] assuming other FCNC couplings to be zero. Note that the LEP2 gives a better limit for  $\kappa_Z^q < 0.52$  and  $\sqrt{|v_Z^q|^2 + |a_Z^q|^2} < 0.32$  than that given by the CDF. From the low energy experiments a more stringent upper bound on the  $tqZ$  couplings  $\sqrt{|v_Z^q|^2 + |a_Z^q|^2} < 0.15$  can be found in [8].

The H1 Collaboration searched for the production processes by considering both of the anomalous vertices  $tu\gamma$  and  $tc\gamma$  from the fact that HERA has much higher sensitivity to  $\kappa_\gamma^u$  than to  $\kappa_\gamma^c$ , due to more favorable parton density [24]. The current limits from HERA are  $\kappa_\gamma^q < 0.19$  (ZEUS) and  $\kappa_\gamma^q < 0.305$  (H1) [25].

In this study we define the branching ratio for FCNC decay of top quark as

$$BR(t \rightarrow qV) = \frac{\Gamma(t \rightarrow qV)}{\sum \Gamma(t \rightarrow qV)}. \quad (5)$$

By convention, we set  $\Lambda = m_t = 175$  GeV and  $\alpha = 1/128$ ,  $\alpha_s = \alpha_s(m_t^2)$  in our calculations. The branching ratios BR of  $t \rightarrow qq$ ,  $t \rightarrow qZ$  and  $t \rightarrow q\gamma$  are shown in Fig. 1. Using the effective lagrangian (1) with the scale  $\Lambda = m_t = 175$  GeV, and standard decay width  $\Gamma(t \rightarrow bW) \simeq 1.4$  GeV, these branchings can be translated into the bounds on the top quark anomalous couplings  $\kappa_\gamma^q < 0.28$ ,  $\kappa_Z^q < 0.77$  and  $\sqrt{|v_Z^q|^2 + |a_Z^q|^2} < 0.48$  as seen in Fig. 1.

The branchings for  $t \rightarrow qZ$  are denoted by the contribution from a 5-dimensional FCNC coupling  $\kappa$  or the 4-dimensional FCNC couplings  $\sqrt{|v_Z^q|^2 + |a_Z^q|^2} = \kappa$  for an illustration. Here, we assume that only the relevant FCNC coupling is allowed to deviate from its SM value at a time as the others are set to zero.

Since we allow  $tc\gamma$  and  $tu\gamma$  anomalous interaction in the direct top quark production we should also include this term in the decay of top quark, which is proportional to  $(\kappa_\gamma^c)^2 + (\kappa_\gamma^u)^2$  and contributes to the top quark decay width. One can see the effect of additional channel for top quark decay, which decreases the  $t \rightarrow bW$  branching ratio and causes a noticeable deviation from the quadratic behavior. Assuming only the presence of  $tc\gamma$  and  $tu\gamma$  couplings top quark decay width changes according to

$$\Gamma_t = \Gamma_{t \rightarrow bW} \left[ 1 + \frac{[(\kappa_\gamma^c)^2 + (\kappa_\gamma^u)^2] \frac{32}{\Lambda^2} m_W^2}{9 (1 - m_W^2/m_t^2)^2 (1 + 2m_W^2/m_t^2)} \right]. \quad (6)$$

While the  $t \rightarrow qV$  ( $q = u, c$  and  $V = \gamma, Z, g$ ) decays will occur in the presence of the anomalous couplings given in Eq. (1), they are smaller than the  $t \rightarrow bW$  decay and they will have negligible branching ratios for  $\kappa_V < 0.2$  at  $\Lambda = m_t$ . Given the existing upper bound of the anomalous coupling mentioned earlier [9],  $t \rightarrow bW$  will be the dominant decay mode of the top quark. Since the leptonic decay channel of W boson has a clear signature, here we consider only the  $t \rightarrow bW^+ \rightarrow l^+\nu b$  decay for our signal.

The total cross section for direct top quark production is given by

$$\sigma = \int_{\tau_{\min}}^{0.83} \int_{\tau/0.83}^1 \frac{dx}{x} f_q(x, Q^2) f_\gamma\left(\frac{\tau}{x}\right) \int_{\hat{t}_-}^{\hat{t}_+} d\hat{t} \frac{d\hat{\sigma}}{d\hat{t}} \quad (7)$$

where  $\hat{t}_- = (m_t^2 - \hat{s})$ ,  $\hat{t}_+ = 0$  and  $\tau_{\min} = m_t^2/s$ . The  $f_\gamma(y)$  is the spectrum of photons scattered backward from the interaction of laser photon with the high energy electrons [28]. The differential cross section for the subprocess  $\gamma q \rightarrow t \rightarrow bW^+$  is given by

$$\frac{d\hat{\sigma}}{d\hat{t}} = \left(\frac{\kappa_\gamma^q}{\Lambda}\right)^2 \frac{\pi\alpha^2|V_{tb}|^2}{9m_w^2\sin^2\theta_w\hat{s}[(\hat{s}-m_t^2)^2+m_t^2\Gamma_t^2]} [\hat{s}^3 + \hat{s}^2\hat{t} - (m_w^2 + 2m_b^2)\hat{s}^2 - (2m_w^2 + m_t^2 + m_b^2)\hat{s}\hat{t} + (m_b^4 + 2m_b^2m_w^2 + 2m_t^2m_w^2)\hat{s} + (m_b^2m_t^2 + 2m_t^2m_w^2)\hat{t} - m_b^2m_t^2m_w^2 - 2m_t^2m_w^4] \quad (8)$$

In this study, the anomalous interaction vertices are implemented into the CALCHEP [25] package with the parton distribution function library CTEQ5M [26] for  $f_q(x, Q^2)$  at  $Q^2 = m_t^2$ . The FCNC  $tq\gamma$  couplings can be probed directly at  $\gamma p$  colliders through the top quark production subprocesses  $\gamma u \rightarrow t$  and  $\gamma c \rightarrow t$ . The diagram for the FCNC top quark production mechanism and its subsequent decay  $t \rightarrow bW^+ \rightarrow l^+\nu b$  are shown in Fig. 2.

The cross sections for anomalous top quark production at three options of  $ep$  colliders with the center of mass energies  $\sqrt{s_{ep}} = 2.64, 3.74$  and  $6.48$  TeV are given in Tables III, III and V, respectively. From these tables it is easy to see that the contribution from  $tu\gamma$  anomalous coupling is larger than that from  $tc\gamma$  coupling.

We search for the signal in detector through the presence of one  $b$ -tagged jet, one isolated lepton and missing transverse momentum. The transverse momentum  $p_T$  distribution of final state particles are given in Fig. 3. The  $b$  quark  $p_T$  distribution has a peak around the half mass of top quark. A small shift backwards due to the mass of final state particles is seen. The  $p_T$  spectrum of the electron (or positron) mainly distributed at the half mass of the  $W$  boson. In Fig. 4 we present the  $p_T$  spectrum of final state particles for the relevant background.

We apply initial kinematic cuts  $p_T^{e,\nu,b} > 10$  GeV for the experimental observation of the signal. These cuts reduce the signal cross section by 5% and background by 45%. More stringent cuts  $p_T^{e,\nu} > 20$  GeV and  $p_T^b > 50$  GeV lead to a reduction on the signal cross section about 50% and background about 85%. The rapidity cuts are more effective such that  $|\eta^{e,\nu,b}| < 2.5$  reduces the signal cross section by a factor about 80% and background by 90%.

In order to enhance the signal to the background, we want to make cuts on the invariant mass of final particles which should be sharply peaked at  $m_t$  for the signal. To determine the invariant mass  $M_{l\nu b}$ , one should reconstruct  $p_t = p_l + p_\nu + p_b$ . The neutrino is not observed but its transverse momentum can be deduced from the missing transverse momentum. The longitudinal component of the neutrino momentum is determined by the  $W$ -mass constraint  $m_W = m_{l\nu} = \sqrt{(p_l + p_\nu)^2}$ , and is given by

$$p_L^\nu = \frac{\chi p_L^l \pm \sqrt{p_l^2(\chi^2 - p_{Tl}^2 p_{T\nu}^2)}}{p_{Tl}^2}, \quad \chi = \frac{m_W^2}{2} + p_T^l \cdot p_T^\nu \quad (9)$$

and  $p_L$  and  $p_T$  refer to the longitudinal and transverse momenta, respectively. We chose the solution which would best reconstruct the mass of the top quark. The invariant mass distributions of  $l\nu b$  system for the three options of anomalous interaction vertex parameters  $\kappa_\gamma^c$  and  $\kappa_\gamma^u$  are shown in Fig. 5 where we apply the cuts  $p_T^{l,\nu,b} > 20$  GeV.

We can determine the minimum value of the anomalous couplings  $\kappa_\gamma^c$  or  $\kappa_\gamma^u$  by using the signal and background events at  $\gamma p$  colliders. Assuming the Poisson statistics the number of signal events required for discovery of a signal at the 95% confidence level is

$$\frac{S}{\sqrt{S+B}} \geq 3 \quad (10)$$

where  $S$  and  $B$  are defined according to the number of events calculation  $(S, B) = \sigma \times BR_w \times L_{int} \times \epsilon$ , where  $\epsilon$  is the overall detection efficiency of 1% for this channel.  $L_{int}$  is the integrated luminosity for one working year, and  $BR_w$  is the branching ratio for leptonic decay of the  $W$  boson.

Since the charm and up quarks are in the initial state, their contributions to direct top quark production can not be distinguished. The plots of the discovery limit when both  $\kappa_\gamma^c$  and  $\kappa_\gamma^u$  are assumed to be nonzero are shown in Figs. 6 and 7.

We find that cross section is more sensitive to  $tu\gamma$  than  $tc\gamma$  due to the more favorable  $u$  quark density in proton. From Fig. 6 one can see that larger center of mass energy improves the sensitivity. Assuming the integrated luminosity of  $100 \text{ fb}^{-1}$  one can probe the anomalous  $tc\gamma$  ( $tu\gamma$ ) couplings down to the value of 0.0095 (0.008) when the scale of the interaction is set to the top quark mass at a CLIC+LHC based  $\gamma p$  collider with  $\sqrt{s_{\gamma p}^{max}} \simeq 5.9$  TeV. For other choices of  $\Lambda$  the results can be rescaled by  $(m_t/\Lambda)^2$ . These limits correspond to the branching ratio  $BR \rightarrow q\gamma \approx 5 \times 10^{-5}$ . In the SM extension with exotic quarks [3],[4] and supersymmetric models with R-parity violation [2], this branching ratio can be as low as  $O(10^{-5})$ . If these models are the only source for the anomalous  $tq\gamma$  couplings, our calculations

therefore indicate that future improvements at the CLIC+LHC based  $\gamma p$  colliders will be needed to make this a detectible signal unless LO and NLO corrections further enhance the contributions.

In principle, there can be the overlapping between the direct top quark production and the photon or gluon splitting diagrams where photon (gluon) splits into a  $q\bar{q}$  pair, and  $u$  and/or  $c$  combines with the gluon (photon) to produce a top quark. Care must be taken with these processes to avoid the double counting. In the direct production due to anomalous  $tc\gamma$  and/or  $tu\gamma$  couplings, initial state particles are assumed to be massless, and thus we may ignore the effects of the double counting problem.

In conclusion, the anomalous couplings can be large in a specific model. The present experimental limits are relatively weak and these couplings can exist in tree level anomalous processes and can be measured with a better precision at high energy lepton-hadron colliders. The FCNC interaction of top quark would be a signal for the existence of new physics beyond the SM.

- 
- [1] B. Grzadkowski, J.F. Gunion and P. Krawczyk, Phys. Lett. B268, 106 (1991); G. Eilam, J.L. Hewett and A. Soni, Phys. Rev. D59, 039901 (1999).
- [2] J.M. Yang, B.-L. Young and X. Zhang, Phys. Rev. D58, 055001 (1998).
- [3] F. del Aguila, J.A. Aguilar-Saavedra and R. Miquel, Phys. Rev. Lett. 82, 1628 (1999).
- [4] J.A. Aguilar-Saavedra and B.M. Nobre, Phys. Lett. B553, 251 (2003).
- [5] D. Atwood, L. Reina And A. Soni, Phys. Rev. D55, 3156 (1997).
- [6] H. Fritzsch, Phys. Lett. B 224, 423 (1989).
- [7] T. Han, R. D. Peccei and X. Zhang, Nucl. Phys. B 454, 527 (1995).
- [8] A. Ahmadov *et al.*, in *Proceedings of the workshop on standard model physics (and more) at the LHC*, Geneva 2000, edited by G. Altarelli and M. L. Mangano, CERN 2000-004, p. 484 (2000).
- [9] T. Han, K. Whisnant, B.-L. Young and X. Zhang, Phys. Lett. B 385, 311 (1996).
- [10] E. Malkawi and T. Tait, Phys. Rev. D 54, 5758 (1996).
- [11] T. Tait and C. P. Yuan, Phys. Rev. D 55, 7300 (1997).
- [12] M. Hosch, K. Whisnant, and B.-L. Young, Phys. Rev. D 56, 5725 (1997).
- [13] T. Han, M. Hosch, K. Whisnant, B.-L. Young and X. Zhang, Phys. Rev. D 58, 073008 (1998).
- [14] T. Tait and C. P. Yuan, Phys. Rev. D 63, 014018 (2001).
- [15] O. Cakir and S. Cetin, ATLAS Internal Note, ATL-COM-PHYS-2002 (2002).
- [16] J.F. Obraztsov, S. Slabospitsky and O. Yushchenko, Phys. Lett. B 426, 393 (1998)
- [17] T. Han, J.L. Hewett, Phys. Rev. D 60, 074015 (1999) .
- [18] H. Fritzsch and D. Holtmannspötter, Phys. Lett. B 457, 186 (1999).
- [19] A. T. Alan and A. Senol, Europhys. Lett., 59, 669 (2002).
- [20] R.W. Assmann *et al.*, The CLIC Study Team, "A 3 TeV  $e^+e^-$  Linear Collider Based on CLIC Technology", CERN 2000-08, Geneva, (2000).
- [21] V. Telnov and H. Burkhardt, "CLIC 3 TeV Photon Collider Option", CERN-SL-2002-013, CLIC Note 508, Geneva, (2002).
- [22] CDF Collaboration, F. Abe *et al.*, Phys. Rev. Lett. 80 (1998) 2525.
- [23] DELPHI Collaboration, P. Abreu *et al.*, Phys. Lett. B446 (1999) 62.
- [24] H1 Collaboration, "Search for single top production in ep collisions at HERA", contributed paper 516, LP2001, Rome.
- [25] S. Dusini, Nucl. Phys. B (Proc. Suppl.), 109B, 262 (2002).
- [26] A. Pukhov *et al.*, hep-ph/9908288 (1999).
- [27] CTEQ Collaboration, H. L. Lai *et al.*, Eur. Phys. J. C12, 375 (2000).
- [28] I.F. Ginzburg *et al.*, Nucl. Instr. and Meth. 205, 47 (1983).

Table I: Branching ratios for FCNC top quark decays as predicted within the SM and the SM extensions.

	$BR(t \rightarrow qg)$	$BR(t \rightarrow q\gamma)$	$BR(t \rightarrow qZ)$
SM	$10^{-10}$	$10^{-12}$	$10^{-13}$
2HDM	$10^{-5}$	$10^{-7}$	$10^{-6}$
SUSY	$10^{-5}$	$10^{-6}$	$10^{-6}$
EXQ	$10^{-3}$	$10^{-5}$	$10^{-2}$

Table II: The main parameters of the options of CLIC+LHC based  $\gamma p$  colliders.

CLIC+LHC	$E_e(\text{TeV})$	$E_p(\text{TeV})$	$\sqrt{s_{ep}}(\text{TeV})$	$\sqrt{s_{\gamma p}^{max}}(\text{TeV})$	$L_{ep} \simeq L_{\gamma p} (\times 10^{32} \text{cm}^{-2} \text{s}^{-1})$
Option 1	0.25	7	2.64	2.41	1-100
Option 2	0.50	7	3.74	3.41	1-100
Option 3	1.50	7	6.48	5.90	1-100

Table III: The cross section for the process  $\gamma p \rightarrow bWX$  at a CLIC+LHC based  $\gamma p$  collider with  $\sqrt{s_{ep}} = 2.64$  TeV.

$\Lambda = m_t$		$\kappa_\gamma^u$						
$\sigma(\text{pb})$		0	0.01	0.05	0.1	0.2	0.3	0.4
$\kappa_\gamma^c$	0	$4.95 \times 10^{-2}$	$1.92 \times 10^{-1}$	$3.61 \times 10^0$	$1.43 \times 10^1$	$5.69 \times 10^1$	$1.28 \times 10^2$	$2.82 \times 10^2$
	0.01	$1.16 \times 10^{-1}$	$3.08 \times 10^{-1}$	$3.73 \times 10^0$	$1.44 \times 10^1$	$5.70 \times 10^1$	$1.28 \times 10^2$	$2.82 \times 10^2$
	0.05	$1.70 \times 10^0$	$2.08 \times 10^0$	$5.50 \times 10^0$	$1.62 \times 10^1$	$5.88 \times 10^1$	$1.29 \times 10^2$	$2.84 \times 10^2$
	0.1	$6.67 \times 10^0$	$6.86 \times 10^0$	$1.03 \times 10^1$	$2.09 \times 10^1$	$6.36 \times 10^1$	$1.35 \times 10^2$	$2.88 \times 10^2$
	0.2	$2.65 \times 10^1$	$2.67 \times 10^1$	$6.68 \times 10^1$	$8.43 \times 10^1$	$1.54 \times 10^2$	$2.69 \times 10^2$	$4.34 \times 10^2$
	0.3	$5.95 \times 10^1$	$1.37 \times 10^2$	$1.43 \times 10^2$	$1.60 \times 10^2$	$2.30 \times 10^2$	$3.46 \times 10^2$	$5.10 \times 10^2$
	0.4	$1.06 \times 10^2$	$2.43 \times 10^2$	$2.49 \times 10^2$	$2.66 \times 10^2$	$3.36 \times 10^2$	$4.52 \times 10^2$	$6.16 \times 10^2$

Table V: The cross section for the process  $\gamma p \rightarrow bWX$  at a CLIC+LHC based  $\gamma p$  collider with  $\sqrt{s_{ep}} = 6.48$  TeV.

$\Lambda = m_t$		$\kappa_\gamma^u$						
$\sigma(\text{pb})$		0	0.01	0.05	0.1	0.2	0.3	0.4
$\kappa_\gamma^c$	0	$2.45 \times 10^{-1}$	$6.33 \times 10^{-1}$	$9.95 \times 10^0$	$3.91 \times 10^1$	$1.55 \times 10^2$	$3.50 \times 10^2$	$6.21 \times 10^2$
	0.01	$5.16 \times 10^{-1}$	$1.15 \times 10^0$	$1.05 \times 10^1$	$3.96 \times 10^1$	$1.55 \times 10^2$	$3.50 \times 10^2$	$6.21 \times 10^2$
	0.05	$6.95 \times 10^0$	$7.58 \times 10^0$	$1.69 \times 10^1$	$4.60 \times 10^1$	$1.62 \times 10^2$	$3.57 \times 10^2$	$6.28 \times 10^2$
	0.1	$2.71 \times 10^1$	$2.77 \times 10^1$	$3.70 \times 10^1$	$6.62 \times 10^1$	$1.82 \times 10^2$	$3.77 \times 10^2$	$6.48 \times 10^2$
	0.2	$1.07 \times 10^2$	$1.08 \times 10^2$	$1.17 \times 10^2$	$1.46 \times 10^2$	$2.62 \times 10^2$	$4.57 \times 10^2$	$7.28 \times 10^2$
	0.3	$2.42 \times 10^2$	$2.43 \times 10^2$	$2.52 \times 10^2$	$2.81 \times 10^2$	$3.97 \times 10^2$	$5.92 \times 10^2$	$8.63 \times 10^2$
	0.4	$4.29 \times 10^2$	$4.29 \times 10^2$	$4.39 \times 10^2$	$4.68 \times 10^2$	$5.84 \times 10^2$	$7.79 \times 10^2$	$1.05 \times 10^3$

Table IV: The cross section for the process  $\gamma p \rightarrow bWX$  at a CLIC+LHC based  $\gamma p$  collider with  $\sqrt{s_{ep}} = 3.74$  TeV.

$\Lambda = m_t$		$\kappa_\gamma^u$						
$\sigma(\text{pb})$		0	0.01	0.05	0.1	0.2	0.3	0.4
$\kappa_\gamma^c$	0	$8.12 \times 10^{-2}$	$2.59 \times 10^{-1}$	$4.52 \times 10^0$	$1.78 \times 10^1$	$7.11 \times 10^1$	$1.59 \times 10^2$	$2.84 \times 10^2$
	0.01	$1.84 \times 10^{-1}$	$4.43 \times 10^{-1}$	$4.70 \times 10^0$	$1.79 \times 10^1$	$7.13 \times 10^1$	$1.59 \times 10^2$	$2.84 \times 10^2$
	0.05	$2.63 \times 10^0$	$2.89 \times 10^0$	$7.15 \times 10^0$	$2.04 \times 10^1$	$7.37 \times 10^1$	$1.62 \times 10^2$	$2.87 \times 10^2$
	0.1	$1.03 \times 10^1$	$1.05 \times 10^1$	$1.48 \times 10^1$	$2.81 \times 10^1$	$8.14 \times 10^1$	$1.69 \times 10^2$	$2.94 \times 10^2$
	0.2	$4.10 \times 10^1$	$4.12 \times 10^1$	$4.55 \times 10^1$	$5.88 \times 10^1$	$1.12 \times 10^2$	$2.00 \times 10^2$	$3.25 \times 10^2$
	0.3	$9.22 \times 10^1$	$9.24 \times 10^1$	$9.67 \times 10^1$	$1.10 \times 10^2$	$1.63 \times 10^2$	$2.51 \times 10^2$	$3.76 \times 10^2$
	0.4	$1.64 \times 10^2$	$1.64 \times 10^2$	$1.68 \times 10^2$	$1.82 \times 10^2$	$2.35 \times 10^2$	$3.23 \times 10^2$	$4.48 \times 10^2$

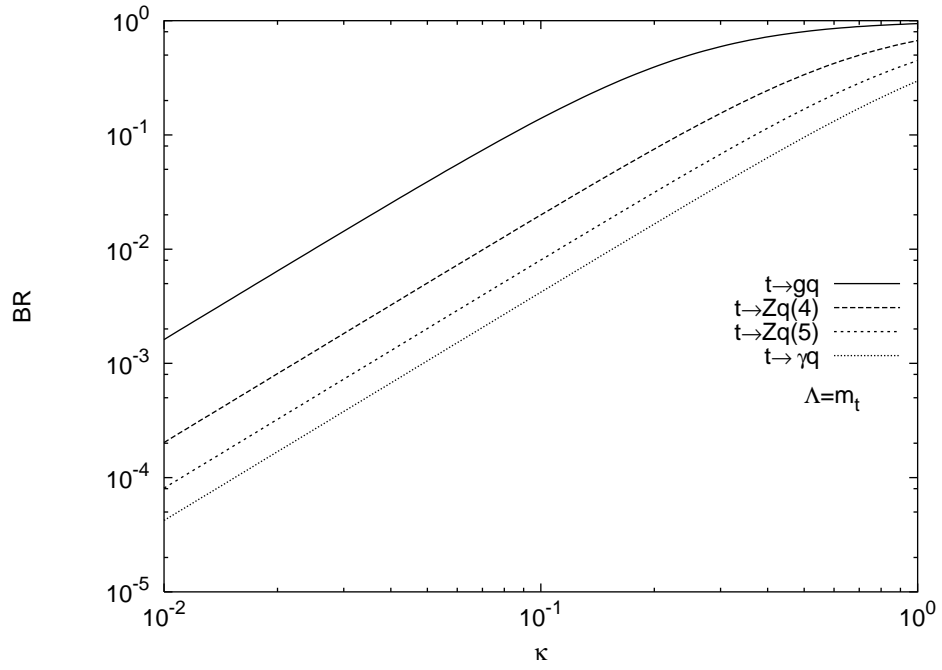


Figure 1: Branching ratios depending on the anomalous coupling  $\kappa$ . Only the relevant FCNC coupling is allowed to deviate from its SM value at a time as the others are set to zero. The branchings  $t \rightarrow qZ$  are considered in two cases as explained in the text.

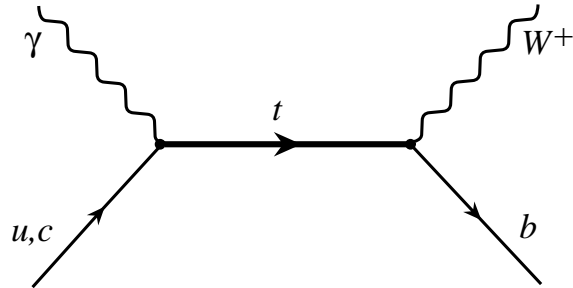


Figure 2: Feynman graph for anomalous top quark production in  $\gamma p$  collision.

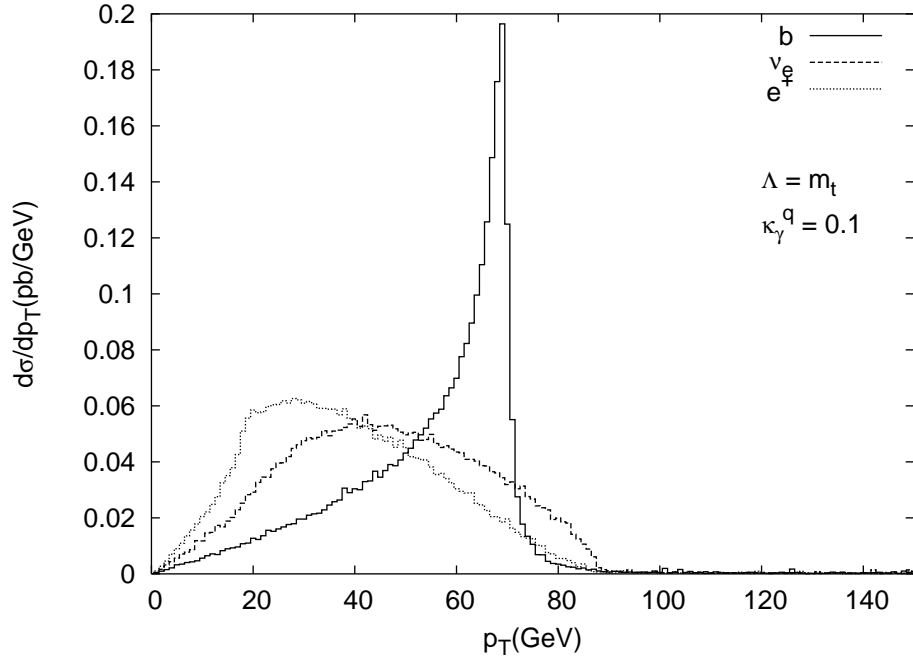


Figure 3: The transverse momentum distribution of  $b$ -quark, lepton ( $e^+$  or  $\mu^+$ ), and the missing  $p_T$  from the FCNC top production at a  $\gamma p$  collider based on CLIC+LHC with  $\sqrt{s_{ep}} = 3.74$  TeV for the scale  $\Lambda = m_t$  and the anomalous coupling  $\kappa_\gamma^q = 0.1$ .

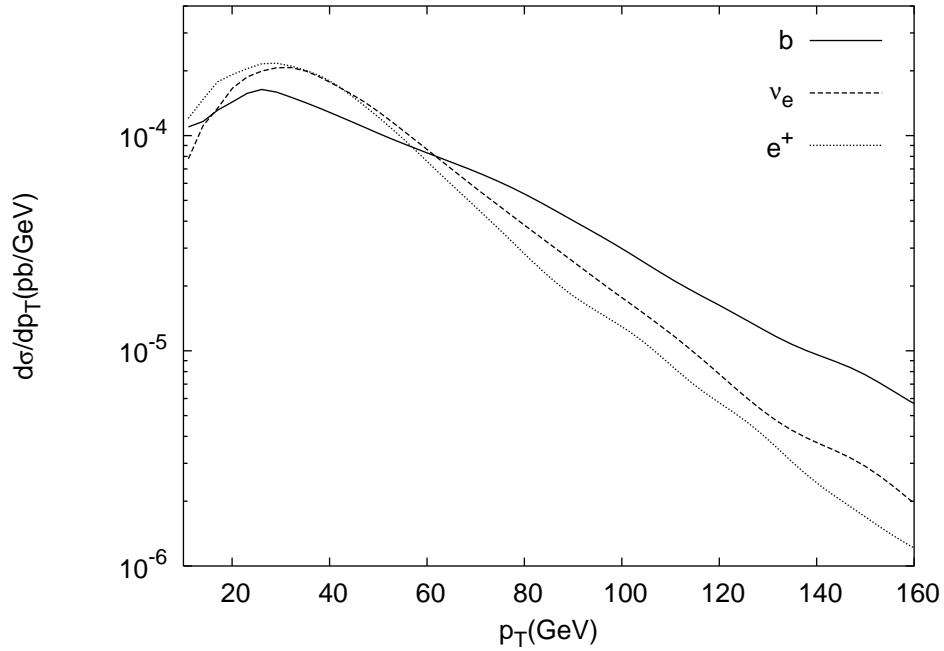


Figure 4: The transverse momentum distribution of  $b$ -quark, lepton ( $e^+$  or  $\mu^+$ ), and the missing  $p_T$  for the process  $ep \rightarrow e^+\nu bX$  at a  $\gamma p$  collider with  $\sqrt{s_{ep}} = 3.74$  TeV.

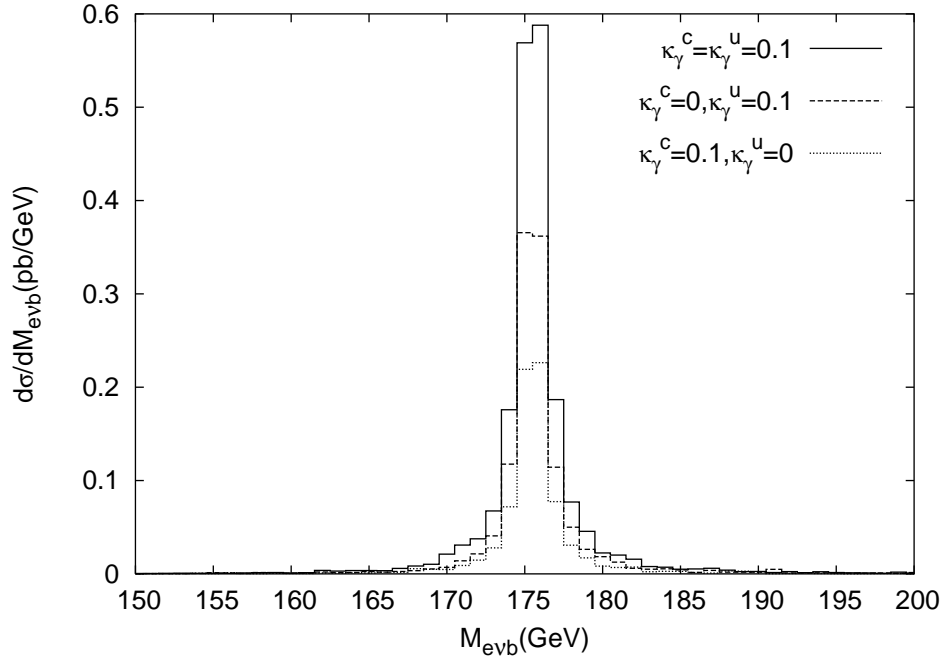


Figure 5:  $M_{evb}$  distributions for the cut  $p_T^{e,\nu,b} > 20$  GeV at the  $\gamma p$  collider with  $\sqrt{s_{ep}} = 3.74$  TeV.

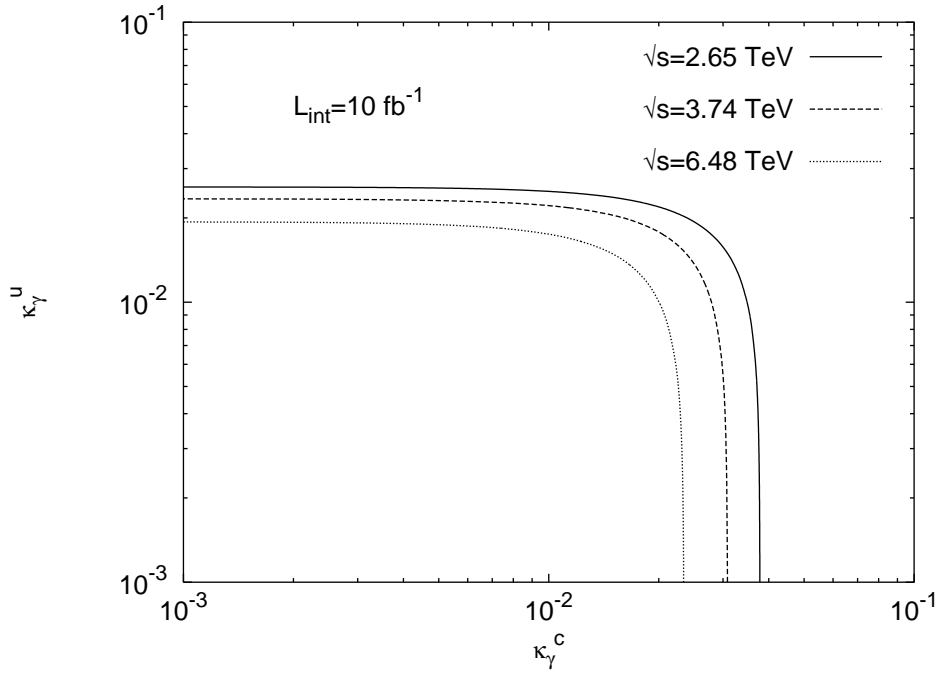


Figure 6: Discovery limits for  $\kappa^c$  and  $\kappa^u$  for each of the colliders considered at  $L = 10 \text{ fb}^{-1}$ , for  $\Lambda = m_t$ .



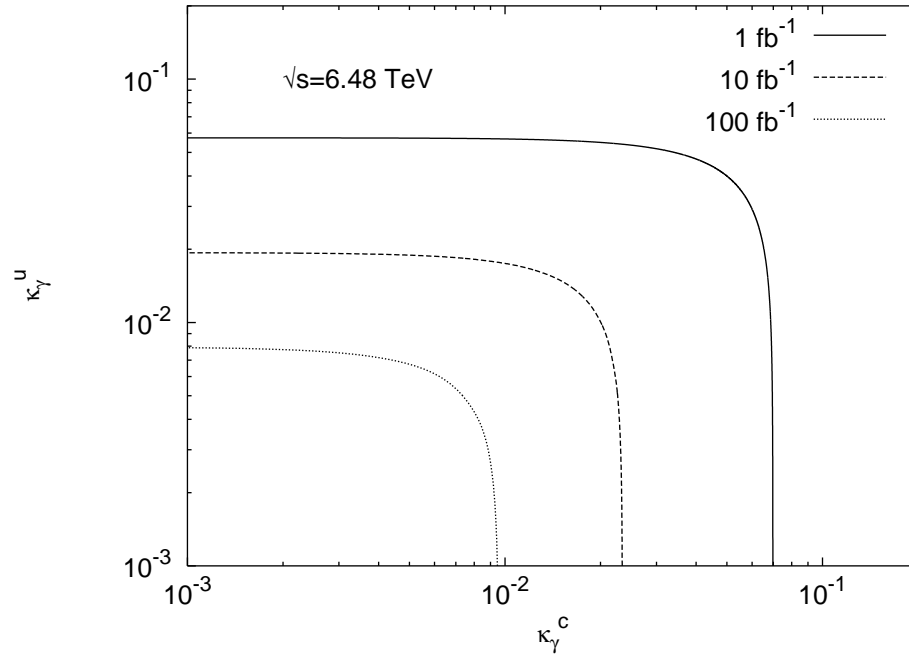


Figure 7: Discovery limits for  $\kappa^c$  and  $\kappa^u$  at CLIC+LHC based  $\gamma p$  colliders at  $\sqrt{s} = 6.48$  TeV for three different luminosity and  $\Lambda = m_t$ .